ANNALI DI GEOFISICA, VOL. XXXVII, N. 3, June 1994

Accurate determination of phase arrival times using autoregressive likelihood estimation

Tormod Kvaerna
NFR/NORSAR, Kjeller, Norway

Abstract
We have investigated the potential automatic use of an onset picker based on autoregressive likelihood estimation. Both a single-component version and a three-component version of this method have been tested on data from events located in the Khibiny Massif of the Kola peninsula, recorded at the Apatity array, the Apatity three-component station and the ARCESS array. Using this method, we have been able to estimate onset times to an accuracy (standard deviation) of about 0.05 s for *P*-phases and 0.15-0.20 s for *S*-phases. These accuracies are as good as for analyst picks, and are considerably better than the accuracies of the current onset procedure used for processing of regional array data at NORSAR. In another application, we have developed a generic procedure to reestimate the onsets of all types of first-arriving *P*-phases. By again applying the autoregressive likelihood technique, we have obtained automatic onset times of a quality such that 70% of the automatic picks are within 0.1 s of the best manual pick. For the onset time procedure currently used at NORSAR, the corresponding number is 28%. Clearly, automatic reestimation of first-arriving *P*-onsets using the autoregressive likelihood technique has the potential of significantly reducing the retiming efforts of the analyst.

Key words *seismology – signal processing – autoregressive analysis – onset time*

1. Introduction

A precise estimate of the onset time of seismic phases is needed to obtain an accurate event location. To obtain very precise onset times for all types of seismic signals, seismological observatories around the world mostly rely on the picks provided by their human analysts. However, the increase in the number of seismic stations worldwide has not been followed up by a similar increase in the number of analysts. The availability and operational use of reliable, automatic procedures therefore become more and more important.

In the automatic detection and signal processing module (SigPro) used for processing the regional array data at NORSAR, a two-step onset time algorithm is in use. This procedure consists of first applying a series of short-term to long-term average (STA/LTA) detectors in parallel to a set of filtered beams. When one or more of the STA/LTA detectors exceed a predefined threshold, a phase detection is declared and a detection time is found. Subsequently, a time domain phase timing algorithm is applied to the filtered beam with the highest SNR, using the detection time as the starting value. A detailed description of this algorithm is found in Mykkeltveit and Bungum (1984).

These SigPro estimates of the onset times are subsequently used by the automatic phase association and event location procedure (ESAL) of the Intelligent Moni-

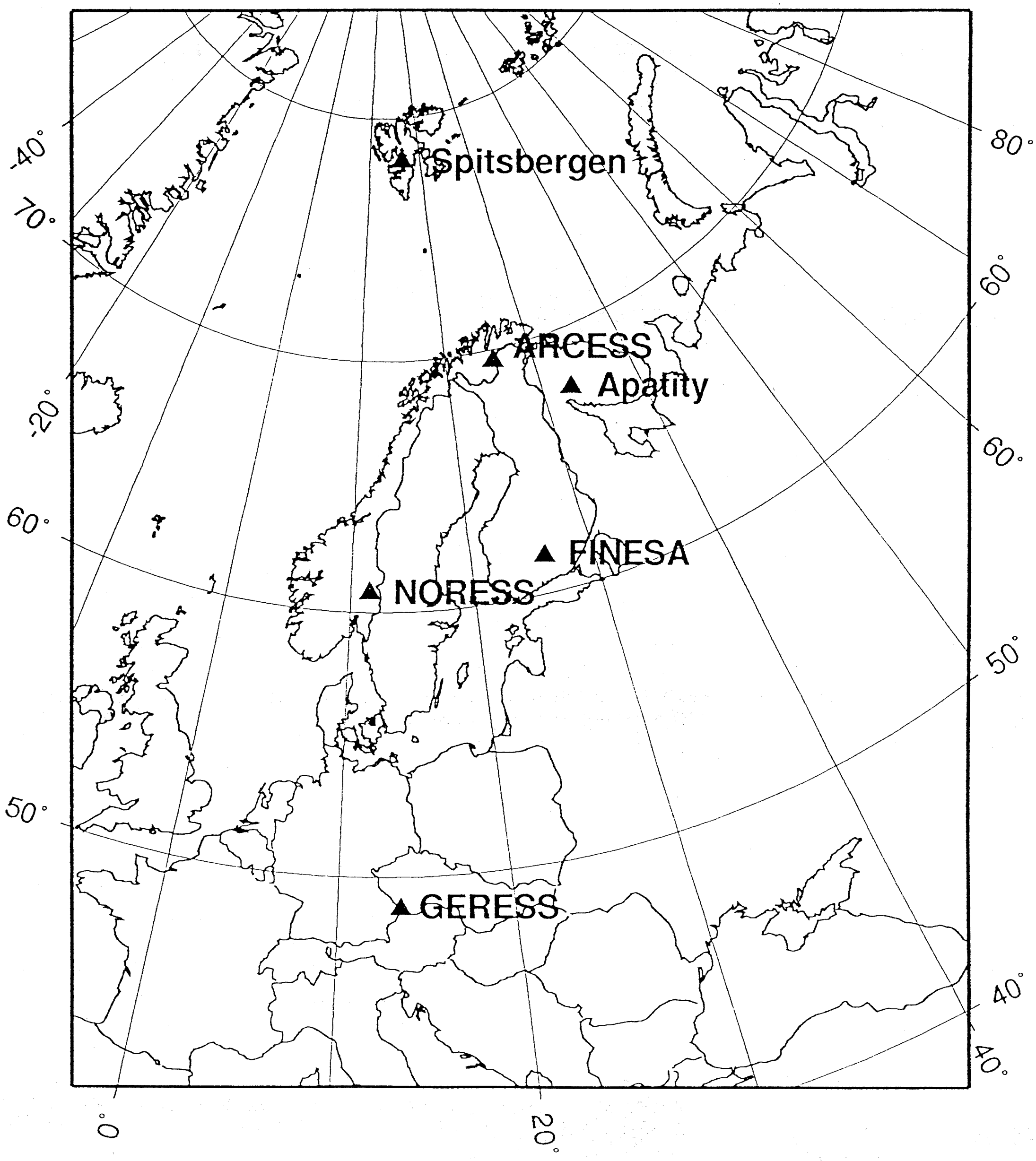

Fig. 1. Map showing the locations of the six regional arrays currently used by the Intelligent Monitoring System at the NORSAR data processing center.

toring System (IMS) (Bache *et al.*, 1993) to produce a fully automatic event bulletin. The IMS currently provides for joint processing of data from six arrays located in Northern and Central Europe, see fig. 1. The events in the automatic bulletin are finally reviewed and corrected by the analyst using the Analyst Review Station (ARS) of the IMS. Through the analyst review we have experienced that the phase onset times often have to be significantly adjusted. In order to improve the precision of the automatic event locations provided by the IMS and in order to reduce the analyst's workload, there is therefore a strong need to improve the precision of the automatic onset time estimates.

Autoregressive modelling has been shown to provide a useful tool in characterizing seismic noise and signals. Tjøstheim (1975a,b) applied such modelling to the seismic discrimination problem. Takanami (1991) used autoregressive models for onset time estimation for microearthquake networks. Pisarenko *et al.* (1987) developed a general autoregressive onset time estimator, which was further elaborated by Kushnir *et al.* (1990). In this study we will investigate the use and performance of this onset time estimation method when applied in an automatic mode under various types of conditions.

2. Autoregressive likelihood estimation of onset time

Following Pisarenko *et al.* (1987) and Kushnir *et al.* (1990), the autoregressive likelihood algorithm for onset time estimation is based on regarding the signal onset as the time when the statistical features of the observed time series are abruptly changed. For each argument τ within a predefined search interval (t_1, t_2) of length N, autoregressive models of the observations within the intervals (t_1, τ) and (τ, t_2) are calculated by a Levinson-Durbin procedure. From the variances σ_1^2 and σ_2^2 of the autoregressive model residuals of the two time intervals, a maximum-likelihood algorithm is used to calculate the likelihood function $L(\tau)$ in accordance with the formula

$$L(\tau) = [\tau ln\sigma_1(\tau) - (N - \tau) ln\sigma_2(\tau)] \tag{2.1}$$

where the argument to the maximum of $L(\tau)$ defines the onset time of the signal, see fig. 2.

The algorithm working on single component data, hereafter denoted ESTON1, takes into account changes in both power and frequency content, and it is therefore important that the broadband signal waveforms are retained. This is very different from the onset time estimator currently used in SigPro, which only exploits power differences within the narrow frequency band with the highest signal-to-noise ratio (SNR). The algorithm working on three-component data, hereafter denoted ESTON3, is in addition sensitive to changes in the polarization characteristics of the three-component observations. Following the recommendations of Pisarenko *et al.* (1987), we have in all our calculations used autoregressive modelling of order 3.

It is noteworthy that both ESTON1 and ESTON3 require that the search be limited to a relatively short time window. If an initial event location and origin time is known, we can determine the required short time window for the search. Alternatively, the phase onsets provided by SigPro can be used to restrict the search. In any case, the autoregressive likelihood estimation of onset time should be well-suited to a post-processing application.

3. Generic application: retiming of first-arriving *P*-phases

This application of post-processing consists of reestimating the onset time of all first-arriving *P*-phases defined in the automatic IMS bulletin, using the ESTON1 method. For a period of four days (September 27-30, 1993), 391 first-arriving *P*-

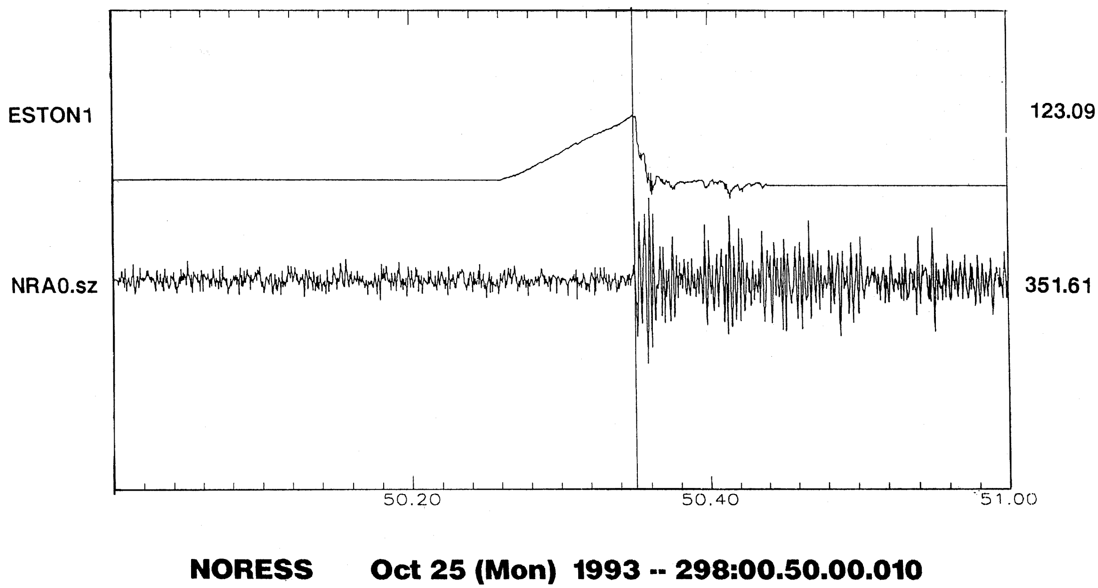

Fig. 2. The top trace is the likelihood function resulting from autoregressive onset time estimation of the data in the bottom trace. The maximum of the likelihood function corresponds to the estimated onset time.

phases associated with events in the IMS bulletin were defined. They were distributed among all the arrays shown in fig. 1, and originated from events at both local, regional and teleseismic distances. All *P*-phases were carefully retimed using an interactive signal processing package (EP) with high-resolution graphics (Fyen, 1989), and about 10% of them were rejected due to false detections or erroneous phase association, such that 350 first-arriving *P*-phases remained for further analysis after this manual screening process. When comparing these numbers to the general IMS performance (Mykkeltveit *et al.,* 1993), it appears that this sample is fairly typical for an operational situation.

The 149 *P*-phases recorded during the two first days of the time period were used to tune the implementation of ESTON1. By comparing the differences between the manual and the SigPro onset times, a maximum difference of 2.8 s was observed. Consequently, the search interval to be used by ESTON1 was set to ±3 s around the SigPro onset.

The different types of *P*-phases (*Pg, Pn, P* and *PKP*) spanned a wide range of signal characteristics with respect to spectral content, complexity, SNR and signature (impulsive, emergent). From extensive testing of ESTON1, we found that in order to successfully process all types of signals, we had to identify the widest possible spectral band for which the signal had usable SNR. This was done in the time domain by estimating the maximum SNR within the search interval in a series of narrow passbands. The spectral band was defined such that we initially selected the narrow frequency band with the highest SNR. If the neighboring frequency bands had an SNR within a factor of 5 of the maximum and also exceeded an SNR of 4, the spectral band was extended so as to include this band as well.

Our experiments also showed that in order to obtain stable estimates of the likelihood function $L(\tau)$, it was important to filter and decimate the data in accordance with the highest frequency of the signal spectrum. For signals with a high SNR (typically above 40) and a wide bandwidth, no filtering or decimation was needed.

We found that the onsets provided by ESTON1 were biased slightly late, and the delay appeared to be linearly dependent on the dominant period of the signal. By linear regression of all signals with SNR > 6, the bias b could be approximated by the relation $b \approx 0.38p$ where p is the dominant period of the signal. The flowchart of fig. 3 outlines the processing steps involved in the reestimation of the arrival time of first-arriving P-phases using the ESTON1 method.

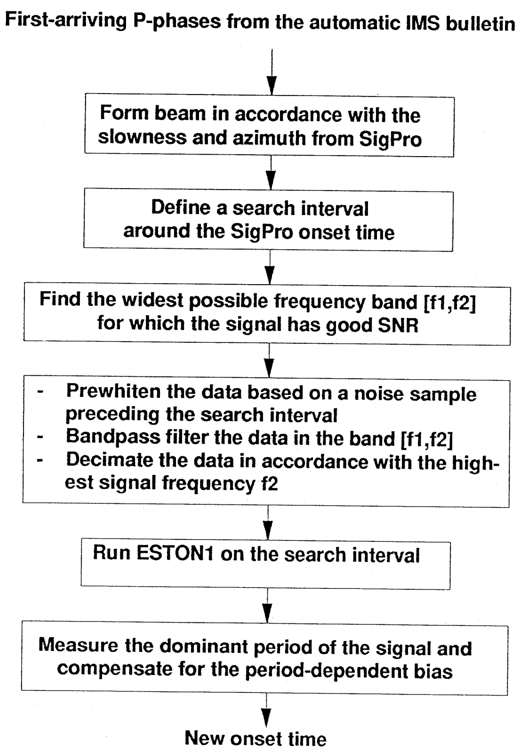

Fig. 3. Flowchart illustrating the processing steps involved in the reestimation of the arrival time of first-arriving P-phases using the ESTON1 method.

The 201 P-phases recorded during the last two days of the test period were used to evaluate the new procedure. Figure 4a shows the difference between the manually picked onsets and the automatic onsets from SigPro versus the highest SNR measured in any narrow filter band. For comparison, fig. 4b shows the difference between the manually picked onsets and the automatically reestimated onset times using the ESTON1 method. From comparing these two figures it is apparent that the improvement when using ESTON1 is significant for all SNRs.

To quantify the improvement, we have plotted in fig. 5 the percentage of the observations within a range of absolute time differences between the automatic and the manual picks. For SigPro, 50% of the automatic onsets were within 0.23 s of the manual pick, whereas for ESTON1 the 50% level (median) was as low as 0.05 s.

We also divided the observations into a teleseismic and a local/regional data set. For SigPro, the median time differences were about equal for the two data sets. For ESTON1, the median time difference was slightly smaller for the local/regional data set than for the teleseismic. This difference could be due to generally longer dominant periods of the teleseismic P-phases.

As expected and also seen from figs. 4a,b, the precision of the automatic onsets is best for high SNRs. By again dividing the observations into two data sets, one with SNR less than or equal to 10 and one with SNR greater than 10, we found that SigPro had a median difference of 0.29 s for the low SNR data set and 0.19 s for the other. The corresponding numbers for ESTON1 were 0.10 s and 0.04 s, respectively.

The implications on the analyst's retiming efforts can be illustrated by the following example: if we assume that the analyst will accept a maximum deviation of 0.1 s from the «correct» manual pick without doing retiming, we can see from fig. 5 that

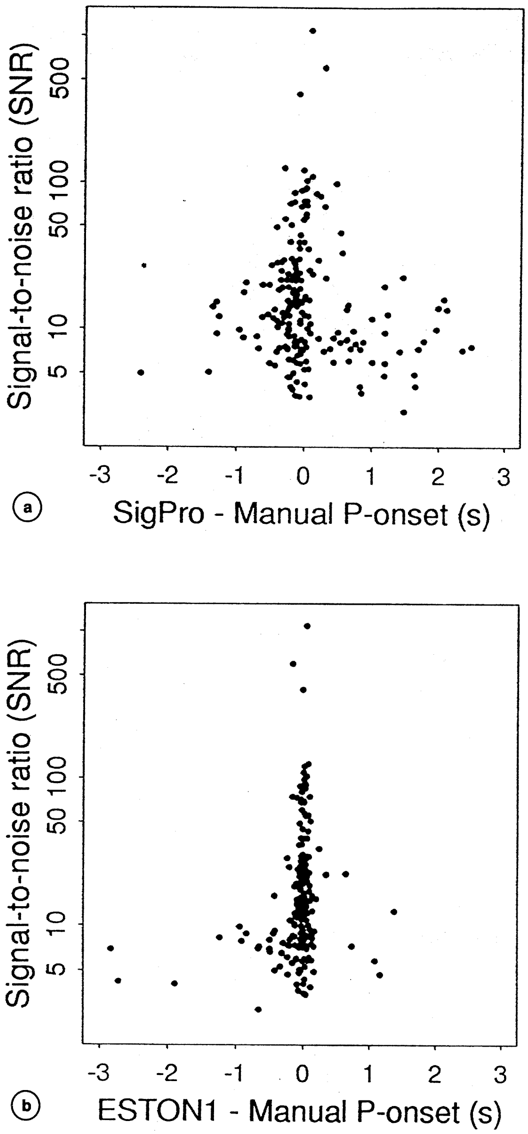

Fig. 4a, b. This figure shows the time difference between the automatic and the manually picked onsets of the 201 first-arriving *P*-phases analyzed in this study plotted versus the SNR of the signal. a) Shows the time differences between the automatic onsets from SigPro and the manual picks. The median absolute time difference is 0.23 s. b) Shows the time differences between the reestimated onsets from ESTON1 and the manual picks. The median absolute time difference is 0.05 s.

28% of the SigPro onsets are acceptable, whereas 70% of the ESTON1 onsets are acceptable. Clearly, automatic reestimation of first-arriving *P*-onsets using the algorithm described above has the potential of significantly reducing the retiming efforts of the analyst.

4. Region-specific application, reprocessing of events from an area with recurring seismicity

The basic principle of region-specific post-processing is to start by subdividing the area to be monitored into smaller regions. For each small region, a set of reference events is analyzed in order to obtain typical features. These characteristics are subsequently utilized when designing an optimum region-specific processing algorithm, which again is activated when an event is located within or close to the actual region. In the following, we will discuss application to a well-calibrated mining area (the Khibiny Massif of the Kola peninsula, Russia) with a high activity rate (Kværna and Ringdal, 1994).

4.1. *The Khibiny Massif events*

Six apatite mines are located within an area of about 10 km^2 in the Khibiny Massif on the Kola peninsula of Russia (see fig. 6). A detailed description of these mines and the mining activity is found in Mykkeltveit (1992). Although we have no explicit information on the exact sizes of these mines, interpretation of various maps suggests that the typical size is about 1 km^2. The Kola Regional Seismological Centre has, since the beginning of 1991, provided NORSAR with information on mining blasts in the six Khibiny Massif mines. The information provided contains an assignment of the relevant mine (1-6), *P* (and normally also *S*) arrival times at the analog APA (Apatity) station (co-located with the three-component station APZ9 of fig. 6),

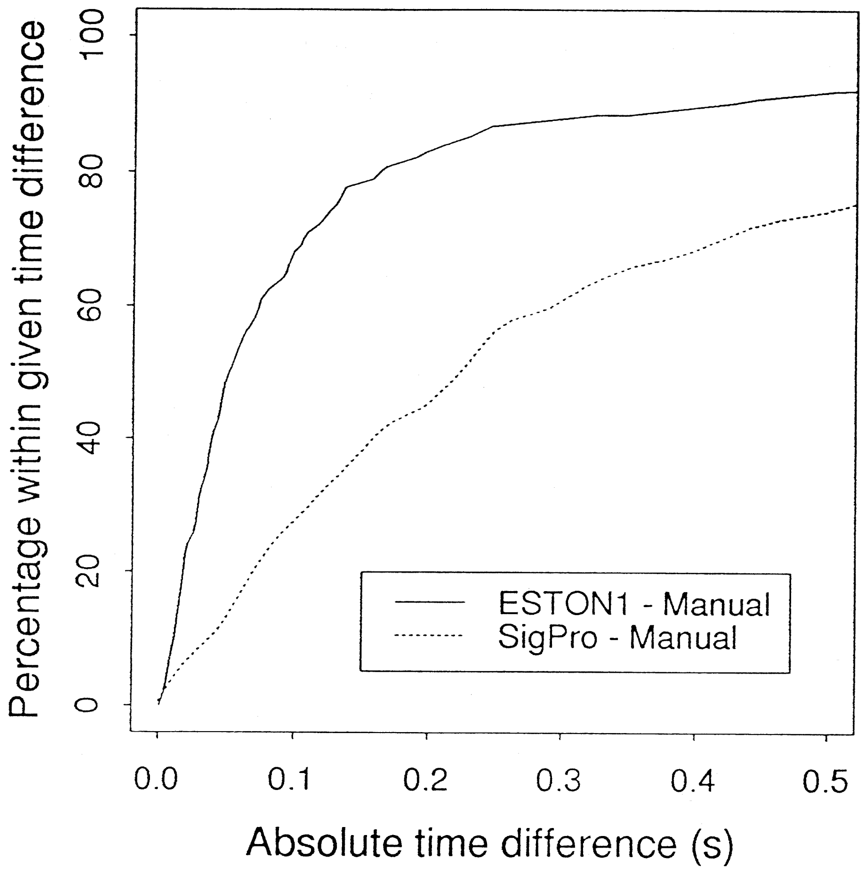

Fig. 5. These two curves show the percentage of the automatic onsets within a range of absolute time differences from the manual picks. For SigPro (dashed line), 50% of the onsets are within 0.23 s of the manual pick, whereas for ESTON1 (solid line) the 50% level (median) is as low as 0.05 s.

the amplitude and period of the signal, and the total charge size in tons. Detailed information on the 58 events used in this study is given in Kværna (1993).

From analysis of the Khibiny mining events recorded at the Apatity array (APA0), the Apatity three-component station (APZ9) and the ARCESS array, several typical characteristics were observed. In order to optimize the automatic algorithm for processing these events, we have utilized different types of characteristic information for each of the three recording stations. We will discuss in the following the details of the retiming sequence that was derived for the Apatity array.

— The Apatity array is located within a distance range of 32-49 km from the different Khibiny mines. For all events, clear *P*, *S* and *Rg* phases are observed.

— The difference between the SigPro *P* onset time and the manual pick were all within ± 2 s. This was the search interval to be used by ESTON1 for reestimating the *P* onsets.

— The *P* signals had generally the best SNR at high frequencies, such that band-

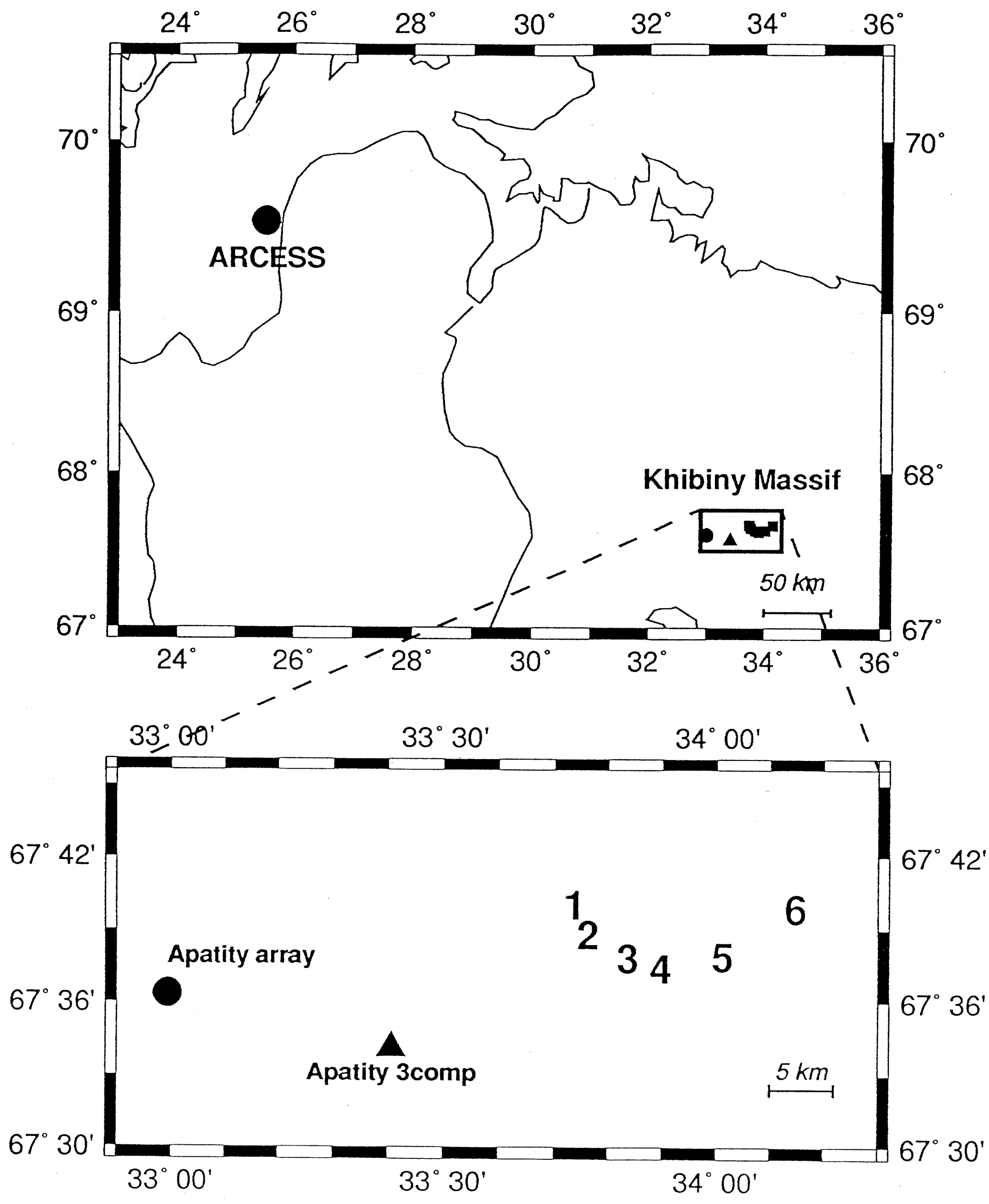

Fig. 6. In the upper part, a large reference area is shown. The location of the ARCESS array is given by a filled circle, and the location of the Khibiny Massif region is shown. The lower part shows a detailed picture of the Khibiny Massif region. The locations of the six mining sites are given by large numbers 1-6. The Apatity array (APA0) is shown as a filled circle and the three-component station (APZ9) in the town of Apatity is shown as a large triangle.

pass filtering and decimation was unnecessary in order to obtain precise onsets by ESTON1. Unlike the generic algorithm for reestimating all types of first-arriving *P*-phases, only prewhitening of the data was needed.

— The peak of the *Rg* phase was identified from an STA envelope created from *z*-component data filtered between 0.8 and 2.0 Hz. The end of the search interval for the *Rg* maximum was conservatively set to 20 s after the *P* onset.

— For estimation of *S*-onsets, the three-component data at the Apatity array was bandpass filtered between 2 and 8 Hz and decimated to 20 Hz sampling. The three-component ESTON3 onset estimator was then applied within a time interval that started 2 s after the *P* onset and stopped at the time of the *Rg* peak.

An illustration of the automatic retiming sequence at the Apatity array is shown in fig. 7, and more details on the retiming sequences for APZ9 and the ARCESS array can be found in Kværna (1993). Note that we were not able to apply the autoregressive likelihood onset time estimator successfully to the *Rg*-phases. We believe that this is primarily due to the surface wave *Rg* not having a well-defined onset like the body waves *P* and *S*.

4.2. *Precision of the onset time estimates*

To evaluate the automatic onset estimates, *P* and *S* onsets at APA0 and APZ9, and the *Pn* onsets at ARCESS were manually picked using the interactive EP program (Fyen, 1989). Given the fact that the characteristics of the Khibiny Massif events were known, the manual phase picking was considered to be done under «optimum conditions». By «optimum conditions» we mean that the analyst utilized information on the approximate phase arrival times and looked for typical signatures of the different phases. We also selected filters and seismometer components to obtain the highest SNR.

In addition, all events were reviewed by another analyst using the Analyst Review Station (ARS) of the IMS. We consider the phase picks from the ARS to be obtained under so-called «operational conditions» and they therefore are less precise than those obtained under «optimum conditions». This is due to the fact that ARS is used as a tool for routine analysis (*i.e.*, relatively short time spent on each pick) of large quantities of data and that the analyst did not have readily available information on the characteristics of the Khibiny Massif events.

Following Sereno (1990), an unbiased estimate of the measurement variance is determined from the arrival time difference between two phase observations for repeated events in the same mine. Specifically:

$$\sigma^2_{1,\mathrm{pick}} + \sigma^2_{2,\mathrm{pick}} = \frac{\sum_{k=1}^{N_{\mathrm{mines}}} \sum_{i=1}^{N_{\mathrm{obs}}} [\Delta T_{\mathrm{obs}_{ik}} - \langle \Delta T_{\mathrm{obs}} \rangle_k]^2}{(N_{\mathrm{obs}} - N_{\mathrm{mines}})} \tag{4.1}$$

where σ_1^2 and σ_2^2 are the picking variance of each phase, $\Delta T_{\mathrm{obs}_{ik}}$ is the *ith* observation of the arrival time difference for the *kth* mine. $\langle \Delta T_{\mathrm{obs}} \rangle_k$ is the mean arrival time difference for the *kth* mine. N_{obs} is the total number of observations (at all mines), and N_{mines} is the number of mines.

We started out by computing the arrival time differences between the manual *P* observations («optimum conditions») for the three stations APA0, APZ9 and ARCESS. The observed arrival time differences were verified to fit a normal distribution using quantile-quantile plots. From three equations of the type above, with altogether three unknowns, we obtained for *P* at APA0 a standard deviation of 0.04 s, for *P* at APZ9 0.06 s and for *Pn* at ARCESS also 0.06 s. In a similar fashion we computed standard deviations for the corresponding automatic picks from the ESTON1 algo-

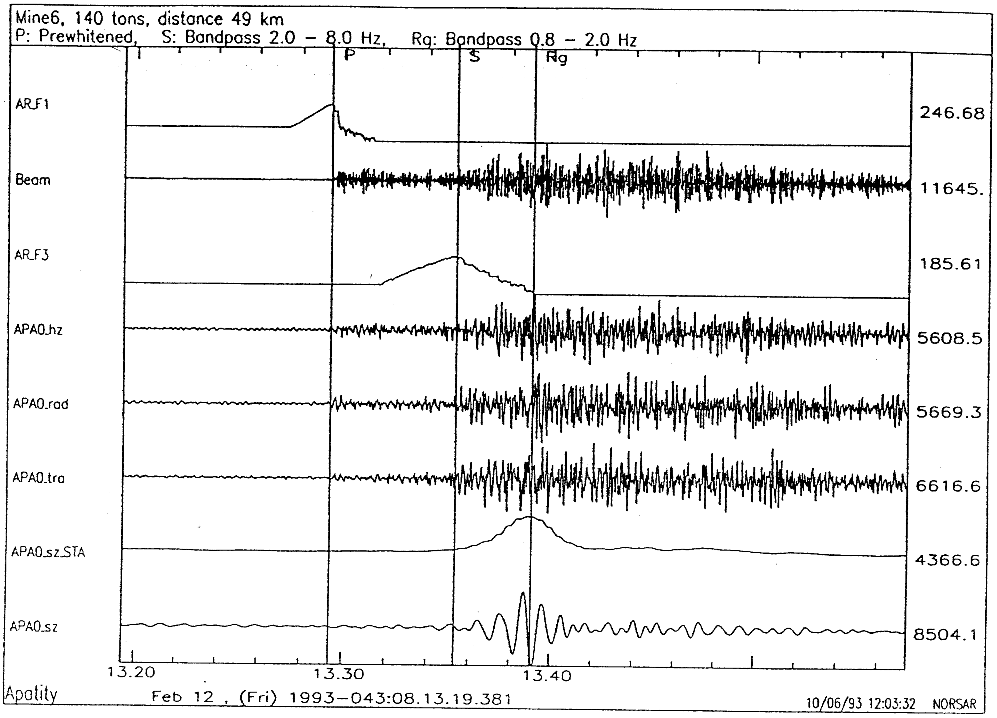

Fig. 7. The seismograms of this figure are Apatity array (APA0) recordings of an event from mine n. 6. The source-receiver distance is 49 km. Trace n. 2 from the top is the prewhitened *P*-beam used for onset-time estimation using ESTON1. The upper trace gives the likelihood function from ESTON1 after processing an interval of ± 2 s around the initial *P*-onset estimate, and the peak of this likelihood function corresponds to the estimated onset. The bottom trace is the vertical component APA0-sz filtered in a low passband (0.8-2.0 Hz) to enhance the *Rg* phase, and the trace above is the STA envelope. The peak of this envelope is declared as the peak of the *Rg* phase. After the *P*-onset and the *Rg* maximum are found, we are searching for the *S*-onset using the three-component ESTON3 estimator. The search interval starts 2 s after the *P*-onset and stops at the *Rg* peak, as seen from the ESTON3 likelihood function of trace n. 3 from the top. The three-component data processed by ESTON3 are given in traces 4-7. Note that there is no need to rotate the three-component data before using ESTON3, but in order to visualize that the *S*-phase has the largest SNR on the transverse component, we have rotated the data. Note that both the ESTON1 and the ESTON3 likelihood functions show clear peaks at the *P*- and *S*-onsets.

rithm. The standard deviations were for *P* at APA0 0.04 s, for *P* at APZ9 0.05 s and for *Pn* at ARCESS also 0.05 s.

It is worth noting that part of the measurement variance is likely to be due to the events of each mine not being located at the same spot, but being distributed within each mine. Under the assumption that each mine has an areal extent 1×1 km (which is reasonable from interpretation of various maps), we have found that the location variability within each mine could have a significant impact on the estimates of the picking precision. With the most unfavorable deployment of the explosions, the influence on σ for the *P*-phases could be as large as 0.05 s. However, all events analyzed in this study originate within a 5 month period, and common mining practice suggests that during such a short time period the mining activity is usually confined to a small portion of each mine. Therefore, it is most likely that the location variability within each mine influence the σ estimates significantly less than 0.05 s. In any case, the results show that for the relatively high frequency and high SNR *P* arrivals analyzed in this study, the automatic ESTON1 method matches the precision of manual picks obtained under «optimum conditions».

To illustrate the improvement in automatic picking precision when using ESTON1 as a part of an intelligent post-processing procedure, we have plotted in fig. 8a the difference between the APA0 *P*-onsets from SigPro and the manual picks obtained under «optimum conditions» as a function of SNR of the signal. Similarly we have plotted in fig. 8b the difference between the *P*-onsets from ESTON1 and the manual picks. From comparing these two figures the improvement, when using ESTON1, is apparent.

For estimating the standard deviations of the other types of onsets we have used a slightly different approach than the one outlined above. Instead of solving three equations of type (4.1) with three unknowns, we have consistently used the manual *P* onset at APA0 («optimum condition») as the reference (with known σ), such that the unknown of the other observation could be directly computed. Table I summarizes the standard deviations for the different types of *P* onsets. Notice that for the three-component station APZ9, no continuous signal processing has been running.

It it seen from table I that the SigPro *P* picks at APA0 ($\sigma \approx 0.27$ s) have a larger scatter than at ARCESS ($\sigma \approx 0.13$ s). One way of explaining this may be that the phase timing procedure has problems for very high frequency signals like *P*-phases at APA0. Another explanation may be that

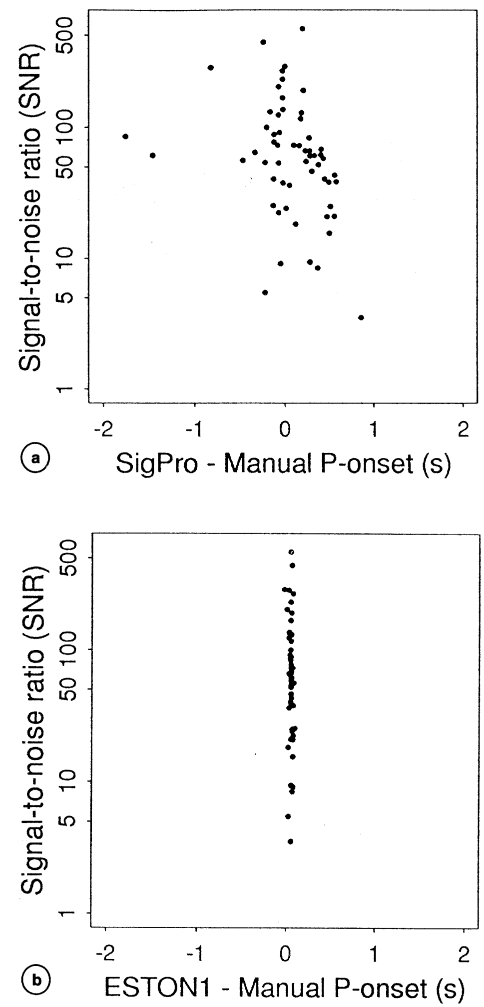

Fig. 8a,b. This figure shows the time differences between the automatic *P*-onsets and the manual picks obtained under «optimum conditions» at APA0 plotted versus the SNR on the prewhitened beam. All 58 *P*-observations are included. a) shows the time differences between the automatic *P*-onsets from SigPro and the manual picks, whereas b) shows the time differences between the automatic *P*-onsets from ESTON1 and the manual picks. In this case, the ESTON1 estimates of the onset times have not been corrected for the period dependent bias of the method. However, due to the consistently high dominant frequencies of the *P*-phases, the correction is very small (less than 0.05 s).

Table I. Standard deviations (σ) for different types of P-onsets. For the automatic SigPro onsets the number of outliers are marked in parenthesis.

	Automatic picks		Manual picks	
	SigPro	ESTON1	Operational conditions (ARS)	Optimum conditions (EP)
APA0	0.27 s (2)	0.04 s	0.05 s	0.04 s
APZ9	—	0.05 s	0.08 s	0.05 s
ARCESS	0.13 s (2)	0.05 s	0.09 s	0.05 s

Table II. Standard deviations (σ) for different types of S-onsets.

	Automatic picks	Manual picks	
	ESTON3	Operational conditions (ARS)	Optimum conditions (EP)
APA0	0.19 s	0.39 s	0.20 s
APZ9	0.15 s	0.18 s	0.13 s

the complex wavetrain at APA0, with P-, S- and Rg-phases arriving within a short time interval, causes problems for the SigPro detector in consistently determining the detection time of the P-phase. However, the precision of the automatic arrival times from ESTON1 are about the same for all stations ($\sigma \approx 0.05$ s). This precision is much better than from SigPro, and even matches the precision of the manual picks obtained during «optimum conditions». The manual picks from ARS («operational conditions») show a somewhat larger scatter than those obtained during «optimum conditions» and illustrate the benefit of having available a priori information when analyzing the events.

In a similar fashion we have estimated the measurement variance of the S-phases at APA0 and APZ9, see table II. Again, the precision of the automatic S-onsets from ESTON3 match the «optimum» manual picks. The automatic onsets at APZ9 ($\sigma = 0.15$ s) are generally more precise than at APA0 ($\sigma = 0.19$ s). We believe this to be due to the more emergent character of S-phases at APA0, which again is a result of generally longer source-receiver distance compared to at APZ9. The manual ARS phase picks are also in this case less precise than those obtained during «optimum conditions», and this is particularly evident at APA0. The S- and Rg-phases at APA0 and APZ9 have a very short time separation (1-3 s) such that during routine operation, the analyst may have difficulties in consistently determining the correct S-onsets, especially when the S-phase is emergent like at APA0. On the other hand, we have during the «optimum» manual phase picking utilized knowledge on the approximate time of the S-arrival such that we could determine the S-onsets more consistently. It would have been interesting to evaluate the precision of the SigPro S-onsets at APA0, but we experienced that the detector had problems when detecting both of two arrivals that had little time separation and large differences in frequency content like the *S*- and *Rg*-phases. In some cases the detector triggered on the *S*-phase, and in other cases on *Rg*. We therefore could not justify including the SigPro *S*-onsets in this comparison.

5. Conclusions

The results presented in this study show that very precise automatic estimates of phase onsets can be obtained with the autoregressive likelihood estimation technique. Implementation of the method requires that we have available approximate estimates of the phase arrival times, and we have shown that such approximate estimates can be obtained from automatic event definitions (phase association and event location) by the Intelligent Monitoring System (IMS). In this way the autoregressive likelihood estimation method can provide phase onsets that match the human precision. This has been demonstrated for events from the Khibiny Massif, by quantifying the uncertainty of both manual and automatic onset estimates of various phases at the Apatity stations and at ARCESS. Furthermore, the precision of the automatic phase picks shows very large improvement in comparison to the automatic phase onsets from the continuous processing providing input to the IMS.

We realize that in order to obtain accurate event locations, precise onset time estimates are necessary, but not sufficient. If the theoretical travel-time model used in the event location deviates from the true travel-times, the accuracy of the event locations will be reduced. Introduction of travel-time corrections as well as other aspects of accurate event location are discussed by Kværna and Ringdal (1994).

During the work with the autoregressive likelihood estimation method, we have experienced that the display of the likelihood functions, as illustrated in fig. 7 can assist the analyst in picking the correct phase onsets. In the context of interactive analysis of seismic data, we believe that the idea of making such likelihood functions available to the analyst should be pursued.

It is clear that when estimating arrival times by the autoregressive method, the results for specific, well-calibrated regions are more precise than can be obtained when the method is used in a «generic» mode. Efforts should be made to extend the number of well-calibrated regions in order to make such optimum use of the method.

Acknowledgements

This research is sponsored by the Advanced Research Projects Agency of the US Department of Defense, and monitored by the Air Force Technical Applications Center under Contract N. F08650-93-C-0002. I would like to acknowledge Dr. A.F. Kushnir for providing the software for onset time estimation and for valuable help when implementing the programs at NORSAR. I would also like to thank Dr. V. M. Trjapitsin of the Kola Regional Seismological Centre for providing the information on the Khibiny Massif events. Discussions with my colleagues Frode Ringdal, Svein Mykkeltveit and Ulf Baadshaug are much appreciated.

NORSAR Contribution N. 501.

REFERENCES

BACHE, T.C., S.R. BRATT, H.J. SWANGER, G.W. BEALL and F.K. DASHIELL (1993): Knowledge-based interpretation of seismic data in the Intelligent Monitoring System, *Bull. Seismol. Soc. Am.*, **83**, 1507-1526.

FYEN, J. (1989): Event processor program package, in *NORSAR Semiannual Tech. Summ. 1 October 1988-31 March 1989*, Scientific Rep. N. 2-88/89, Kjeller, Norway.

KUSHNIR, A.F., V.M. LAPSHIN, V. I. PINSKY and J. FYEN (1990): Statistically optimal event detection using small array data, *Bull. Seismol. Soc. Am.*, **80** (part B), 1934-1950.

KVAERNA, T. (1993): Intelligent post-processing of seismic events – part 2: Accurate determination of phase arrival times using autoregressive likelihood estimation, in *NORSAR Semiannual Tech. Summ. 1 October 1992-31 March 1993*, Scientific Rep. N. 2-92/93, Kjeller, Norway.

KVAERNA, T. and F. RINGDAL (1994): Intelligent post-processing of seismic events, *Annali di Geofisica*, **37** (3), 309-322.

MYKKELTVEIT, S. and H. BUNGUM (1984): Processing of regional seismic events using data from small-aperture seismic arrays, *Bull. Seismol. Soc. Am.*, **74**, 2313-2333.

MYKKELTVEIT, S. (1992): Mining explosions in the Khibiny Massif (Kola peninsula of Russia) recorded at the Apatity three-component station, *Report PL-TR-92-2253*, Phillips Laboratory, Hanscom AFB, MA, U.S.A.

MYKKELTVEIT, S., U. BAADSHAUG, B.KR. HOKLAND, T. KVÆRNA and L.B. LOUGHRAN (1993): An evaluation of the performance of the Intelligent Monitoring System, in *NORSAR Semiannual Tech. Summ. 1 October 1992-31 March 1993*, Scientific Rep. N. 2-92/93, Kjeller, Norway.

PISARENKO, V.F., A.F. KUSHNIR and I.V. SAVIN (1987): Statistical adaptive algorithms for estimation of onset moments of seismic phases, *Phys. Earth Planet. Int.*, **47**, 4-10.

SERENO, T.J. (1990): Attenuation of regional phases in Fennoscandia and estimates of arrival time and azimuth uncertainty using data recorded by regional arrays, *Semiannual Tech., Rep. N. 3, 1 January 1989-30 June 1990*, Science Applications International Corp., San Diego, CA, U.S.A.

TAKANAMI, T. (1991): A study of detection and extraction methods for microearthquake waves by autoregressive models, *Journal of the Faculty of Science, Hokkaido University Series VII (Geophysics)*, **9** (1).

TJØSTHEIM, D. (1975a): Some automatic models for short-period noise, *Bull. Seismol. Soc. Am.*, **65**, 677-691.

TJØSTHEIM, D. (1975b): Autoregressive representation of seismic *P*-wave signals with an application to the problem of short-period discriminants, *Geophys. J.R. Astron. Soc.*, **43**, 269-291.